NANO LETTERS

2003
Vol. 3, No. 5
589−592

Anomalously Immobilized Water: A New Water Phase Induced by Confinement in Nanotubes

R. Jay Mashl,*,†,‡,§ Sony Joseph,† N. R. Aluru,†,||,⊥,○,# and Eric Jakobsson†,‡,§,||,●,▽

Beckman Institute for Advanced Science and Technology, National Center for Supercomputing Applications, Center for Biophysics and Computational Biology, Bioengineering Program, General Engineering Department, Department of Electrical and Computer Engineering, Department of Mechanical and Industrial Engineering, Department of Molecular and Integrative Physiology, and Department of Biochemistry, University of Illinois, Urbana, Illinois 61801

Received January 13, 2003; Revised Manuscript Received March 21, 2003

ABSTRACT

Confinement can induce unusual behavior in the properties of matter. Using molecular dynamics simulations, we show here that water confined to carbon nanotubes of a critical size under ambient conditions (1 bar, 300 K) can undergo a transition into a state having icelike mobility with an amount of hydrogen bonding similar to that in liquid water. The onset of this behavior occurs rapidly, raising the possibility that confinement inside nanotubes, and perhaps even buckyballs, can provide an environment in which the dynamics of phase changes may be studied directly by simulation. Moreover, because of a variety of evidence suggesting that water ordering may modulate proton conductance via a "proton wire" hydrogen bonding network, the ability to modulate water ordering with geometry suggests a possible mechanism for a switchable nanoscale semiconductor.

Since their discovery,[1] carbon nanotubes have been the subject of many studies, including those investigating their physical and chemical properties.[2] Because they resemble elongated cylindrical sheets of graphite, the notion of nanotubes as containers and conduits has existed for several years. Nanotube occupation by water entering from open ends was originally suggested[3] theoretically as a wetting phenomenon, and since then it not only has been observed computationally in molecular dynamics (MD) simulations[4−6] but also has been strongly suggested experimentally by the fact that the fluorescence of nanotubes embedded in lipid micelles is affected by the pH of the external electrolyte.[7] Here we study both the structure and dynamics of water confined within carbon nanotubes of various sizes using MD simulations under ambient conditions. We find that whereas the water generally shows slowed dynamics compared to that of the bulk, in nanotubes of a critical diameter it forms a structure resembling a stack of cyclic water hexamers exhibiting properties characteristic of both hexagonal ice and liquid water.

* Corresponding author. E-mail: mashl@uiuc.edu.
† Beckman Institute for Advanced Science and Technology.
‡ National Center for Supercomputing Applications.
§ Center for Biophysics and Computational Biology.
|| Bioengineering Program.
⊥ General Engineering Department.
○ Department of Electrical and Computer Engineering.
Department of Mechanical and Industrial Engineering.
● Department of Molecular and Integrative Physiology.
▽ Department of Biochemistry.

Methods. We embedded uncapped, single-walled carbon nanotubes of various diameters (see Table) into wafers composed of neutral atoms mimicking the hydrophobic interior of a phospholipid membrane and filled the empty space with water molecules. Carbon nanotubes (length about 40 Å), ranging from 3.1 to 18.1 Å in diameter as measured between van der Waals surfaces of opposing nanotube atoms, were placed in a dielectric wafer composed of neutral atoms that extended approximately 20−25 Å laterally. Periodic boundary conditions were implemented in all three directions. Bulk SPC/E water, having atomic charges of −0.8476*e* and 0.4238*e* on oxygen and hydrogen, respectively, was equilibrated at 300 K and then used to fill the nanotube interiors and interwafer regions. Molecular dynamics simulations were performed using a 2-fs time step. The tube and wafer atoms were held stationary while the water temperature was regulated at 300 K using a modified Nosé−Hoover thermostat (time constant 0.5 ps). Pressure normal to the wafer was maintained at 1 bar using a modified Parrinello−Rahman piston-coupling scheme (time constant 20 ps; compressibility 4.5×10^{-5} bar^{-1}). Values for the Lennard-Jones interaction parameters for the nanotube ("C"), wafer ("S"), and water oxygen ("O") were $\sigma_{CC} = 3.36$ Å, $\epsilon_{CC} = 0.0970$ kcal mol^{-1}; $\sigma_{OC} = 3.26$ Å, $\epsilon_{OC} = 0.123$ kcal mol^{-1}; and $\sigma_{OS} = 3.52$ Å, $\epsilon_{OS} = 0.135$ kcal mol^{-1}, respectively, and were group-based with a 15-Å cutoff. Electrostatic interactions used the

10.1021/nl0340226 CCC: $25.00
Published on Web 04/08/2003

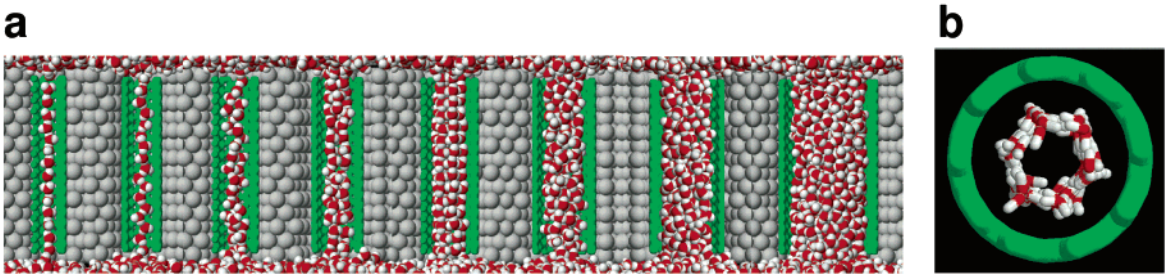

Figure 1. Snapshots from molecular dynamics simulations at 300 K. (a) Composite image of all systems (see Table) with nanotube size increasing from left to right. In narrow nanotubes, the water adopts a single-file arrangement but becomes more disordered in a fashion similar to that of bulk water in wider nanotubes. Confined within a nanotube of a "critical" diameter (fifth from left), the water spontaneously orders into a regular array. (b) Cross-sectional view of water inside the critical-sized 8.6-Å-diameter nanotube showing a multicolumnar water structure. Colors: nanotube (green), wafer (gray), water oxygens (red), water hydrogens (white). Images were derived from visualizations using RasMol.

Table 1. Nanotube Geometries[a]

carbon nanotube geometry	van der Waals diameter (Å)
(5, 5)	3.1
(6, 6)	4.5
(7, 7)	5.9
(8, 8)	7.2
(9, 9)	8.6
(10, 10)	9.9
(12, 12)	12.6
(16, 16)	18.1

[a] Lattice vectors describing the armchair nanotubes studied (C−C bond length, 1.42 Å) and their corresponding cross sections.

particle-mesh Ewald method with a 10-Å real-space cutoff, a 1.5-Å reciprocal space gridding, and splines of order 4 with a 10^{-5} tolerance. The SETTLE algorithm was used to constrain the geometry of the water molecules. The data shown here are from equilibrated MD trajectories lasting approximately 2 ns. Results for hydrogen bonding and water diffusion were based on 300-ps intervals at a 50-fs sampling rate, and those pertaining to dipole autocorrelation were based on 30-ps intervals at a 10-fs sampling rate. Water molecules entering or exiting a nanotube during an interval were disregarded. All simulations were done with the GROMACS software package.[8] A given simulation contained 2500 to 4500 water molecules, depending on the size of the nanotube being simulated. The amount of water was sufficient for bulklike water properties to be found away from the entrance to the nanotube.

With regard to the validation of methods, the SPC/E water model[9] was originally designed to reflect the dielectric constant and self-diffusion coefficient of liquid water accurately. In our laboratory, we have found that this model accurately tracks the self-diffusion coefficient of liquid water over the entire range of temperature from 0 to 100 °C (S.-W. Chiu, unpublished results). Gay et al.[10] have done extensive simulations of ice properties with the SPC/E model and found an accurate representation of ice structure, compressibility, and variation of density with temperature. The freezing temperature of SPC/E water is within a few degrees of the experimental value. Those authors noted that this quality of behavior depends on an appropriate treatment of the long-range forces by Ewald sums, which we have utilized in this paper. Our group has previously considered carefully the effects of various aspects of the molecular dynamics computational method on the behavior of simulated water.[11] We have also successfully replicated complex behaviors of water in interaction with biomolecules, including the successful simulation of the water permeability of the gramicidin channel in a lipid bilayer[12] and the effects of varying hydration levels on the structure of a lipid bilayer.[13] On the basis of our experience and that of other workers, we believe that all aspects of the simulation methods in this paper represent "best practices" in molecular dynamics of systems that include water and organic or biological molecules.

Results. Snapshots of the systems equilibrated under ambient conditions (300 K, 1 bar) show (Figure 1) that in the narrowest nanotube the water molecules adopt a single-file formation with a 1D hydrogen bonding pattern, as has been reported on in earlier molecular dynamics simulations,[4] whereas in the wider nanotubes they appear to be more disordered. However, in the nanotube with a diameter of 8.6 Å (for a (9,9)-armchair nanotube), they are transformed into a highly ordered lattice filling the hydrophobic cavity.

When viewed along the nanotube axis (Figure 1b), this water appears to be arranged as a stacked column of cyclic hexamers, the building block of the I*h* phase of ice[14] with both intra- and intercolumnar hydrogen bonding. In recent experimental studies, cyclic water hexamers have been characterized[15] by infrared spectroscopy in liquid helium droplets at temperatures near absolute zero, have been seen to form on palladium[16] and copper[17] surfaces, and have been found[18] by X-ray crystallography to be present within the gaps (about 9 Å × 6 Å wide) of an organic host crystal at 173 K. The significance of our observation is to show the possibility of the confinement-induced formation of an array of stacked cyclic water hexamers at 300 K.

To examine the hydrogen bonding capability of the water inhabiting the nanotubes (Figure 2), a hydrogen bond was said to exist if the candidate water molecules were both inside the tube, the donor−acceptor distance was within 3.5 Å, which is the first minimum of the radial distribution function for water oxygens in bulk water, and the orientation of the O−H donor bond was within 60° of the acceptor oxygen.

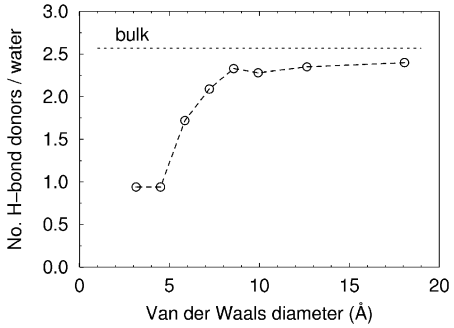

Figure 2. Average number of hydrogen bond donors per water among water molecules found inside the nanotubes at 300 K. The reference value for bulk water was computed to be 2.6.

We find that just under one donating hydrogen bond per water on average is present in the narrowest tube, consistent with there being virtually no discontinuities in the hydrogen bonding chain. As the nanotube diameter increases (as does the cavity volume), the mean number of hydrogen bond donors per water increases and then plateaus at the critical diameter at a value of 2.4. This value is distinctly larger than the optimal value of two for bulk ice and is nearly equal to the bulk value of 2.6. Thus, the confined water has structural properties simultaneously similar to both bulk ice and bulk water.

With regard to dynamic properties, we computed the mean-square distance (MSD) traversed by the center of masses of individual water molecules. The MSD is defined as $\langle|\Delta\mathbf{r}(t)|^2\rangle = \langle|\mathbf{r}(t) - \mathbf{r}(0)|^2\rangle$, where $\mathbf{r}$ denotes the center-of-mass coordinates, t is the time interval, and the angle brackets denote an average over water molecules. The mean-square displacement (MSD) of these water molecules (Figure 3a) shows that the critical 8.6-Å diameter nanotube virtually immobilizes the water. This behavior is expressed in terms of a diffusion coefficient along the axis, defined by Einstein's relation to be equal to half the slope of the MSD curve at long times (taken here as 15 ps $\leq t \leq$ 40 ps). The resulting diffusion coefficients, normalized to that of bulk water, are shown in Figure 3b. The axial diffusion coefficient of water in the critical (9, 9) nanotube in particular was found to be 1.4×10^{-6} cm^2 s^{-1}. On the basis of an MSD analysis, water is found to flow more slowly through nanotubes than in bulk water.

We then examined the reorientability of solvent inside the nanotubes using an autocorrelation function (ACF) for the water dipoles. The ACF is given as $C(t) = \langle\mathbf{p}_i(0)\cdot\mathbf{p}_i(t)\rangle/\langle p^2\rangle$, where $\mathbf{p}$ is the water−water dipole moment (magnitude 2.35 D) and the angle brackets denote averages over time t and molecules. The results, graphed in Figure 4, reveal the following qualitative features. For the wider nanotubes, the ACFs generally take on a bulklike character. However, for the smaller nanotubes, the appearance of plateaus suggests that hydrogen bonds tend to form particularly rapidly (time scale, <1 ps) and be maintained for much longer. Notably, the 8.6-Å diameter nanotube shows here the largest degree of water rotational immobilization, suggesting a relaxation time that is likely to be on a time scale of a larger order of magnitude. The fact that these same water molecules tend

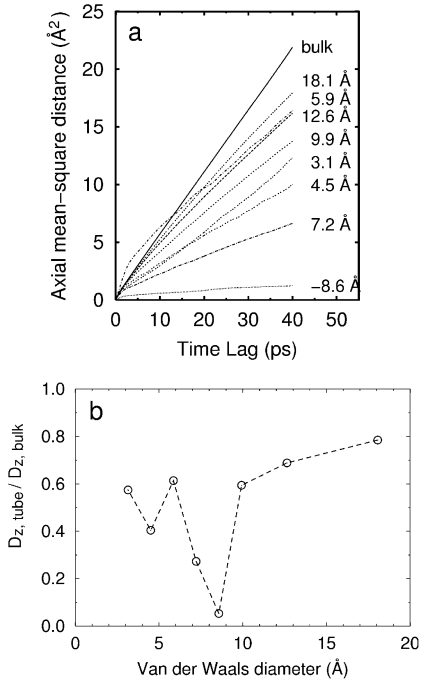

Figure 3. Water mobility inside nanotubes at 300 K. (a) Mean-square displacement (MSD) of water traveled along the nanotube axis for the various nanotubes in the Table. (b) Axial diffusion coefficient of water, normalized to bulk (2.69×10^{-5} cm^2 s^{-1}), derived from panel a.

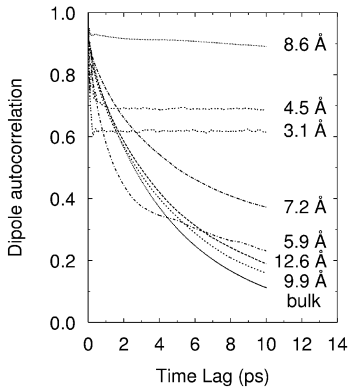

Figure 4. Water reorientation dynamics inside nanotubes at 300 K. Shown is the water dipole autocorrelation function for various nanotubes in the Table. Data for the 18.1-Å nanotube was indistinguishable from that of the bulk.

to translate very slowly even at 300 K implies that their rotational motions, happening within a narrow range of angles, occur rather frequently and very rapidly. The water essentially "quivers" while slowly translating.

We conclude that water motions and orientations are qualitatively modified by confinement in the nanometer-scale regions inside nanotubes. Confinement as seen here generally causes the water dynamics to be consistently slower than that seen in the bulk. In a nanotube of critical size, the water displays anomalous icelike behavior in both symmetry and mobility while retaining a liquidlike degree of water−water hydrogen bonding. These results thus suggest that the confined water is in an intermediate state having both solid- and fluidlike properties.

Proton conduction in different channels varies widely in its efficiency. (For a review, see ref 19.) Proton mobility is high in narrow channels such as gramicidin[20−23] or certain synthetic ion channels[24] in which water arranged in an obligatory single file[25−28] forms a continuous "proton wire". However, aquaporin water channels have a special conformation in the narrow part of their channels that disrupts the regular hydrogen-bonded "proton wire" water configuration,[29−31] resulting in a high permeability to water but not to protons. Among other proteinaceous channels, colicin has an anomalously high proton conductivity.[32] The diameter of the narrowest region of colicin Ia channels has been estimated[33] to be 7 Å and is fairly close to the 8.6-Å nanotube diameter that causes anomalous water ordering in our simulations.

The dependence of proton conduction on water order and of water order on the confining geometry raises an interesting possibility for the design of nanosemiconductors. In considering current carriers for devices at this size scale, we note that electrons have the disadvantage of readily being able to tunnel across distances of nanometers, and as a result, it may be difficult to distinguish between the "on" and "off" states of a such a device. However, protons in water, tunneling readily just a couple of angstroms per "hop" between adjacent water molecules in an ordered state, have appealing properties by providing a current density that is higher than that of other ions[34] and by being able to have the proton mobility switched off by some relatively subtle perturbation that disrupts the water order.

Acknowledgment. Work on this project was supported by grants from the National Science Foundation, the National Institutes of Health, the Defense Advanced Research Projects Agency, and by a computer-time grant from the National Center for Supercomputing Applications.

References

(1) Iijima, S. *Nature (London)* **1991**, *354*, 56.
(2) Dresselhaus, S.; Dresselhaus, G.; Avouris, P.; Eds., *Carbon Nanotubes: Synthesis, Structure, Properties, and Applications*; Springer: Berlin, 2001; Vol. 80.
(3) Dujardin, E.; Ebbesen, T. W.; Hiura, H.; Tanigaki, K. *Science (Washington, D.C.)* **1994**, *265*, 1850.
(4) Hummer, G.; Rasaiah, J. C.; Noworyta, J. P. *Nature (London)* **2002**, *414*, 188.
(5) Koga, K.; Gao, G. T.; Tanaka, H.; Zeng, X. C. *Nature (London)* **2001**, *412*, 802.
(6) Noon, W. H.; Ausman, K. D.; Smalley, R. E.; Ma, J. *Chem. Phys. Lett.* **2002**, *355*, 445.
(7) O'Connell, M. J.; Bachilo, S. M.; Huffman, C. B.; Moore, V. C.; Strano, M. S.; Haroz, E. H.; Rialon, K. L.; Boul, P. J.; Noon, W. H.; Kittrell, C.; Ma, J. P.; Hauge, R. H.; Weisman, R. B.; Smalley, R. E. *Science (Washington, D.C.)* **2002**, *297*, 593.
(8) Lindahl, E.; Hess, B.; van der Spoel, D. *J. Mol. Model.* **2001**, *7*, 306.
(9) Berendsen, H. J. C.; Grigera, J. R.; Straatsma, T. P. *J. Phys. Chem.* **1987**, *91*, 6269.
(10) Gay, S. C.; Smith; E. J.; Haymet, A. D. J. *J. Chem. Phys.* **2002**, *116*, 8876.
(11) Chiu, S.-W.; Clark, M.; Subramaniam, S.; Jakobsson, E. *J. Comput. Chem.* **2000**, *21*, 121.
(12) Chiu, S.-W.; Subramaniam, S.; E. Jakobsson. *Biophys. J.* **1999**, *76*, 1939.
(13) Mashl, R. J.; Scott, H. L.; Subramaniam, S.; Jakobsson. E. *Biophys. J.* **2001**, *81*, 3005.
(14) Hobbs, P. V. *Ice Physics*; Clarendon: Oxford, 1974.
(15) Nauta, K.; Miller, R. E. *Science (Washington, D.C.)* **2000**, *287*, 293.
(16) Mitsui, T.; Rose, M. K.; Fomin, E.; Ogletree, D. F.; Salmeron, M. *Science (Washington, D.C.)* **2002**, *297*, 1850.
(17) Morgenstern, K.; Rieder, K.-H. *J. Chem. Phys*. **2002**, *116*, 5746.
(18) Custelcean, R.; Afloroaei, C.; Vlassa, M.; Polverejan, M. *Angew. Chem., Int. Ed*. **2000**, *39*, 3094.
(19) Decoursey, T. E. *Physiol. Rev*. **2003**, *83*, 475.
(20) Cukierman, S. *Biophys. J.* **2000**, *78*, 1825.
(21) Gowen, J. A.; Markham, J. C.; Morrison, S. E.; Cross, T. A.; Busath, D. D.; Mapes, E. J.; Schumaker, M. F. *Biophys. J*. **2002**, *83*, 880.
(22) Akeson, M.; Deamer, D. W. *Biophys. J.* **1991**, *60*, 101.
(23) Busath, D. D.; Szabo, G. *Biophys J.* **1988**, *53*, 697.
(24) Lear, J. D.; Wasserman, Z.; DeGrado, W. F. *Science (Washington, D.C.)* **1988**, *240*, 1177.
(25) Levitt, D. G. *Curr. Top. Membr. Transp*. **1984**, *21*, 181.
(26) Pomès, R.; Roux, B. *Biophys. J.* **1996**, *71*, 19.
(27) Chiu, S. W.; Subramaniam, S.; Jakobsson, E. *Biophys. J.* **1999**, *76*, 1939.
(28) Eisenman, G.; Enos, B.; Hägglund, J.; Sandblom, J. *Ann. N.Y. Acad. Sci.* **1980**, *339*, 8.
(29) de Groot, B. L.; Grubmuller, H. *Science (Washington, D.C.)* **2001**, *294*, 2353.
(30) Kong, Y. F.; Ma, J. P. *Proc. Natl. Acad. Sci. U.S.A.* **2001**, *98*, 14345.
(31) Tajkhorshid, E.; Nollert, P.; Jensen, M. O.; Miercke, L. J. W.; O'Connell, J.; Stroud, R. M.; Schulten, K. *Science (Washington, D.C.)* **2002**, *296*, 525.
(32) Kienker, P.; Slatin, S. L.; Finkelstein, A. *Biophys. J.* **2002**, *82*, 555a (abstract).
(33) Krasilnikov, O. V.; Da Cruz, J. B.; Yuldasheva, L. N.; Varanda, W. A.; Nogueira, R. A. *J. Membr. Biol.* **1998**, *161*, 83.
(34) Robinson, R. A.; Stokes, R. H. *Electrolyte Solutions*; Butterworth: London, 1959.

NL0340226